Journal of Hepatocellular Carcinoma Dovepress

Open Access Full Text Article ORIGINAL RESEARCH

Predicting Pathological Response of Neoadjuvant Conversion Therapy for Hepatocellular Carcinoma Patients Using CT-Based Radiomics Model

Haoxiang Wen[1,2,*], Ruiming Liang[3,*], Xiaofei Liu[4], Yang Yu[1], Shuirong Lin[1], Zimin Song[1], Yihao Huang[1], Xi Yu[1], Shuling Chen[5], Lili Chen[6], Baifeng Qian[1], Jingxian Shen[7], Han Xiao[8], Shunli Shen[1]

[1]Center of Hepato-Pancreatico-Biliary Surgery, The First Affiliated Hospital of Sun Yat-Sen University, Guangzhou, Guangdong Province, People's Republic of China; [2]Department of Hepatobiliary Surgery, National Cancer Center/National Clinical Research Center for Cancer/Cancer Hospital and Shenzhen Hospital, Chinese Academy of Medical Sciences and Peking Union Medical College, Shenzhen, Guangdong Province, People's Republic of China; [3]Department of Medical Statistics, Clinical Trials Unit, The First Affiliated Hospital of Sun Yat-Sen University, Guangzhou, Guangdong Province, People's Republic of China; [4]Department of Gastroenterology, The First Affiliated Hospital of Sun Yat-senUniversity, Guangzhou, Guangdong Province, People's Republic of China; [5]Precision Medicine Institute, the First Affiliated Hospital of Sun Yat-Sen University, Guangzhou, Guangdong Province, People's Republic of China; [6]Department of Pathology, The First Affiliated Hospital of Sun Yat-Sen University, Guangzhou, Guangdong Province, People's Republic of China; [7]Department of Radiology, Sun Yat-Sen University Cancer Center, State Key Laboratory of Oncology in South China, Collaborative Innovation Center for Cancer Medicine, Guangzhou, Guangdong Province, People's Republic of China; [8]Division of Interventional Ultrasound, The First Affiliated Hospital of Sun Yat-sen University, Guangzhou, Guangdong Province, People's Republic of China

*These authors contributed equally to this work

Correspondence: Shunli Shen, Center of Hepato-Pancreatico-Biliary Surgery, The First Affiliated Hospital of Sun Yat-sen University, No. 58 Zhong-Shan Road2, Guangzhou, Guangdong Province, People's Republic of China, Email Shenshli@mail.sysu.edu.cn; Han Xiao, Division of Interventional Ultrasound, The First Affiliated Hospital of Sun Yat-sen University, No. 58 Zhongshan Road2, Guangzhou, Guang- Dong Province, People's Republic of China, Email xiaoh69@mail.sysu.edu.cn

Purpose: Predicting the pathological response after neoadjuvant conversion therapy for initially unresectable hepatocellular carcinoma (HCC) is essential for surgical decision-making and survival outcomes but remains a challenge. We aimed to develop a radiomics model to predict pathological responses.

Methods: We included 203 patients with HCC who underwent hepatectomy after neoadjuvant conversion therapy between 2015 and 2023 and separated them into a training set (100 patients from Center A) and a validation set (103 patients from Center B). Pathological complete response (pCR)-related radiomic features were extracted from the largest tumor layer in the arterial and portal vein phases of the CT. A synthetic minority oversampling technique (SMOTE) was used to balance the minority groups in the training set. The SMOTE radiomics model was constructed using a logistic regression model in the SMOTE training set and its performance was verified in the validation set.

Results: The AUC of the preoperative modified response evaluation criteria in solid tumors (mRECIST) assessment for pCR was 0.656 and 0.589 in the training and validation sets, respectively. The SMOTE radiomics model was established based on ten radiomic features and showed good pCR-predictive performance in the SMOTE training set (AUC, 0.889; accuracy, 87.7%) and the validation set (AUC: 0.843, accuracy: 86.4%). The RFS of the radiomics-predicted-pCR group was significantly better than that of the predicted-non-pCR group in the training cohort (P = 0.001, 2-year RFS: 69.5% and 30.1% respectively) and the validation cohort (P = 0.012, 2-year RFS: 65.9% and 38.0% respectively).

Conclusion: The SMOTE radiomics model has great potential for predicting pathological response and evaluating RFS in patients with unresectable HCC after neoadjuvant conversion therapy.

Keywords: hepatocellular carcinoma, radiomics, pathological complete response, neoadjuvant conversion therapy

Received: 17 July 2024
Accepted: 18 October 2024
Published: 1 November 2024

Introduction

Hepatocellular carcinoma (HCC) is one of the most common primary malignant tumors of the liver and its incidence is on the rise globally.[1] Surgical resection is the best choice for long-term survival of patients with HCC.[2,3] However, 70–80% of HCC patients in China are already in the middle or advanced stage at initial diagnosis and have lost the opportunity for surgery, with the 5-year survival rate is less than 20%.[4]

Neoadjuvant conversion therapy refers to local or systemic treatment (transarterial chemoembolization(TACE), hepatic arterial infusion chemotherapy(HAIC), tyrosine kinase inhibitors (TKIs), immune checkpoint inhibitors (ICIs), etc.) to transform initially unresectable HCC into resectable HCC for surgical opportunity. The long-term clinical benefit of hepatectomy after neoadjuvant conversion therapy is significantly improved in patients with advanced HCC. The 5-year recurrence-free survival (RFS) was approximately 11.5% compared with 5.6% for hepatectomy directly.[5]

Whether pathological complete response (pCR) is achieved after neoadjuvant conversion therapy is critical for the prognosis of advanced HCC.[6,7] However, pathological response could only be accurately assessed with postoperative specimens. The preoperative prediction of pCR remains challenging. The modified Response Evaluation Criteria in Solid Tumors (mRECIST) is one of the most recommended and commonly used criteria for assessing tumor response.[8] However, a previous study showed that the agreement rate between the mRECIST assessment of CR and pathologic assessment of pCR was only 67.4%.[9] Therefore, predicting the pathological response before surgery remains a challenge.

The information obtained from standard imaging patterns usually refers to simple features such as the shape, size, and contrast enhancement of the tumor. However, radiomics could mine a large number of invisible high-order features that have been shown to provide insight into tumor phenotypes and spatial heterogeneity.[10–12] Many studies have demonstrated the application value of radiomics in challenging clinical problems.[11,13] It has been extensively studied in HCC. For instance, it has been used to predict MVI and other high-risk factors affecting postoperative recurrence before surgery.[14] It can also predict the prognosis of different treatments, optimize the choice of treatment before surgery,[15] and predict the pathological types and immune status of HCC.[16] This indicates that radiomics plays an important role in predicting the pathological types of tumors, evaluating patient prognosis, and selecting treatment options.

Therefore, we aimed to develop a radiomics model based on contrast-enhanced CT(CECT) radiomics features to predict postoperative pathological responses in surgical patients after neoadjuvant conversion therapy.It might able to guide the development of neoadjuvant conversion therapy protocols and the timing of surgery.

Patients and Methods

Patients

This study included 203 patients with initially unresectable HCC who underwent hepatectomy after neoadjuvant conversion therapy at two independent centers. The flowchart is shown in Figure 1. The inclusion criteria were as follows: (1) HCC was confirmed by pathology; (2) The tumor was considered unresectable due to advanced HCC or insufficient residual liver volume after surgery; (3) hepatectomy after neoadjuvant conversion therapy, such as TACE, HAIC, TKIs, and ICIs; (4) CECT examination performed 1 month before hepatectomy; and (5) >18 years old. The exclusion criteria were as follows: (1) Non-HCC confirmed by pathology, (2) Combined with other malignant tumors, and (3) No CECT examination performed 1 month before hepatectomy.

The efficacy of neoadjuvant conversion therapy was evaluated using mRECIST criteria.[8] pCR was defined as the absence of surviving tumor cells in postoperative tumor specimens under sufficient sampling conditions. RFS was defined as the period from the date of hepatectomy to the date of recurrence or metastasis. Data collection, clinical assessments, and neoadjuvant conversion therapy protocols are described in the Supplementary Materials.

The study strictly complied with the Declaration of Helsinki and was approved by the Ethics Committee of the First Affiliated Hospital of Sun Yat-sen University (Approval Number:2023[399]). The requirement for written informed consent was waived by the institutional review board since the study was based on retrospective data, and all data were generated from clinical routine. And all information related to patient privacy or indentification has been desensitized.

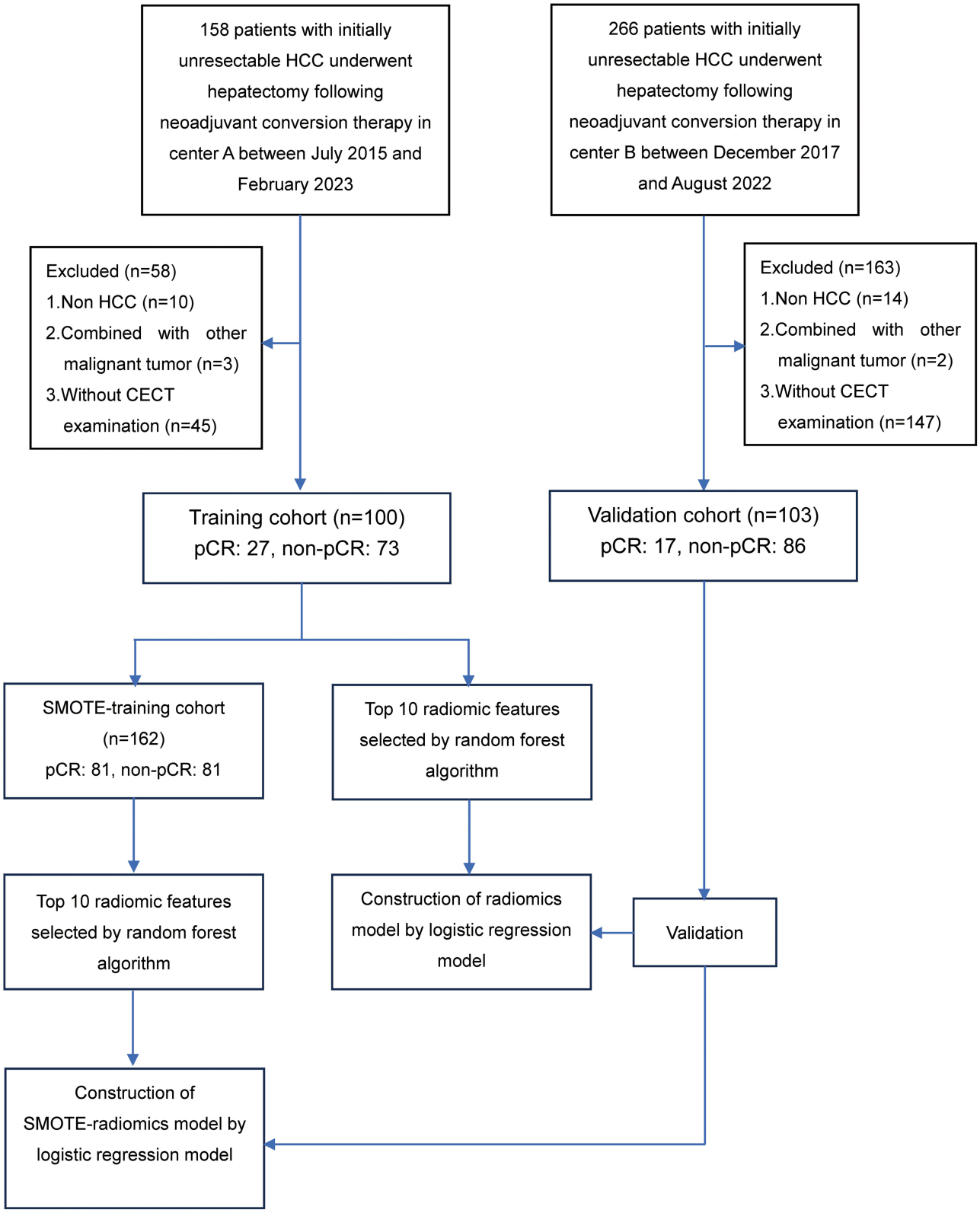

Figure 1 Flow chart of this study.
Abbreviations: HCC, hepatocellular carcinoma; pCR, pathological complete response; SMOTE, synthetic minority over-sampling technique.

Segmentation of Tumor Regions of Interest(ROIs) and Radiomic Features Extraction

The ROIs were hand-plotted on the largest cross-sections of the largest tumors in the arterial and portal vein phases of preoperative CECT by two radiologists using the Analysis-Kit software by 2 radiologists (Figure 2). All ROIs were collated by a senior radiologist and disagreements were resolved unanimously. The Analysis-Kit software automatically extracted 396 radiomic features from each ROI.

Data Balancing and Radiomics Model Construction

In the training set, there was an imbalance in the ratio of patients with pCR to those without pCR, with a ratio of 1:3.07 (27 pCR and 83 non-pCR patients). To address this imbalance, we employed the synthetic minority oversampling technique (SMOTE) algorithm, resulting in a balanced 1:1 ratio (81 pCR patients and 81 non-pCR patients) in the SMOTE-training set.[17] The SMOTE method was not used for the external independent validation group. Before applying the oversampling approach, we conducted data preprocessing, which included removing highly correlated features with Spearman correlation coefficient or Pearson's coefficient greater than 0.90, and data standardization.[18]

To achieve a more effective radiomics model, we established two models: the SMOTE radiomics model based on the SMOTE training set, and the radiomics model based on the original training set. Both the models were subsequently evaluated using a validation set (Figure 1). The random forest algorithm was adopted to select the top-10 features according to their importance, and logistic regression was applied to construct the radiomics model. Each patient's radiomic score was calculated based on the selected radiomic features weighted by their coefficients.

Multiple model evaluation metrics, including AUC, sensitivity, specificity, and accuracy, will be assessed to comprehensively select the model that performs best as the final radiomics model. The highest Youden index was used as the optimal cut-off value for the radiomic model score to divide the patients into predicted pCR and non-pCR subgroups. In addition, five-fold cross-validation was applied for robust estimation in both the training set and SMOTE training set. The SMOTE radiomics model score was equal to the sum of the normalized data for each feature multiplied by the corresponding coefficient minus the constant term of 0.836. The cut-off value was 0.2109.

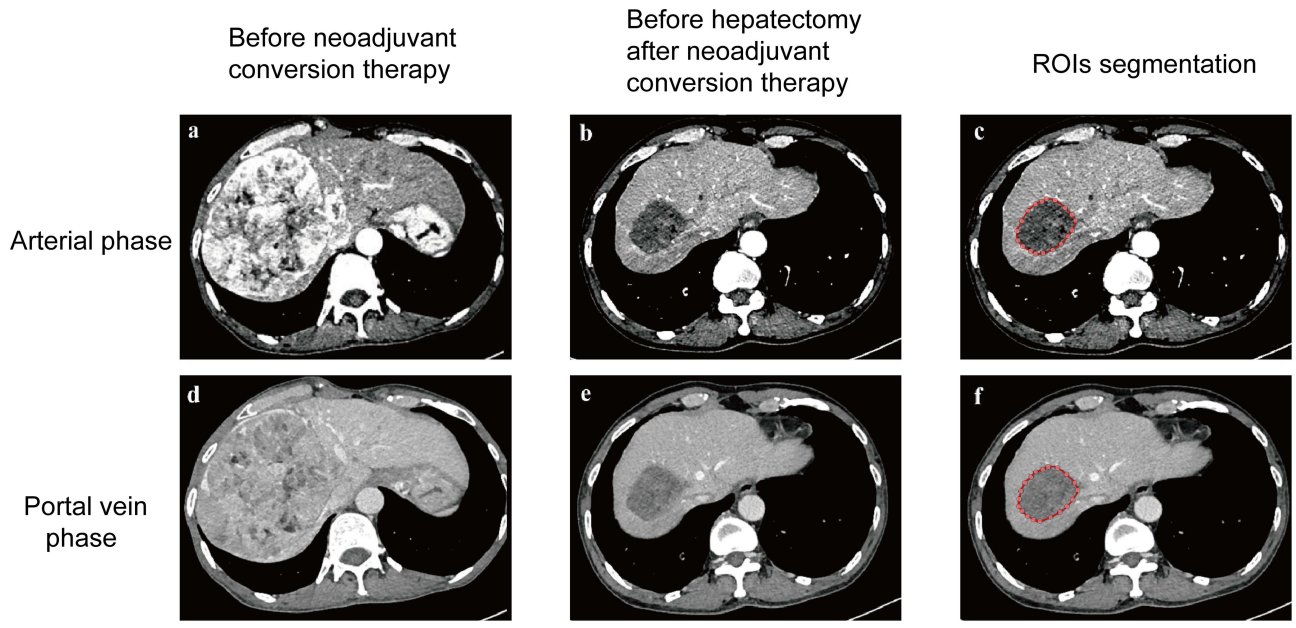

Figure 2 Representative contrast-enhanced CT images of an initially unresectable hepatocellular carcinoma patient with pathological complete response following by neoadjuvant conversion therapy. Arterial phase (**a**) and portal vein phase image (**d**) before neoadjuvant conversion therapy. Preoperative arterial phase (**b**) and portal vein phase image (**e**) after neoadjuvant conversion therapy. Hand-plotted ROI from preoperative arterial phase (**c**) and portal vein phase image (**f**) after neoadjuvant conversion therapy.

Abbreviation: ROI, region of interest.

Determining the Final Predictive Model

Combined with the predicted pCR based on the selected radiomics model, the pCR-associated clinical characteristics ($P < 0.1$ were selected for the construction of the clinical radiomics model by logistic regression. The mRECIST model was developed based on preoperative assessments by radiologists. We compared the performance of these three models (selected radiomics (radiomics model or SMOTE radiomics model, select one model which performs better as the selected radiomics model), clinical-radiomics, and mRECIST models) in both training and validation sets. Clinical-radiomics and mRECIST models were constructed based on original training set. If the addition of clinical variables did not significantly improve the AUC over the radiomics model, and the radiomics model significantly outperformed the mRECIST model, the radiomics model was chosen as the final predictive model for this study.

Statistical Analysis

Continuous variables were described using either mean and standard deviation or median and interquartile range, and comparisons were made using the Student's *t*-test or Wilcoxon rank-sum test, depending on the results of the normality tests. Categorical variables are expressed as numbers and proportions and were assessed using either the chi-square test or Fisher's exact test. Survival curves between the two groups were generated using the Kaplan-Meier method and compared using the Log rank test. Logistic regression was used to analyze the factors associated with pCR, while Cox regression was used to analyze the factors associated with RFS. The Delong's test was used to compare the areas under the ROC curve (AUCs). Statistical significance was set at $P < 0.05$ (two tailed) was considered statistically significant. All statistical analyses were conducted using the R statistical software (version 4.1.1, https://www.r-project.org/) and SAS software (version 9.4; SAS Inc., Cary, N.C., USA).

Results

Clinicoradiological Characteristics

A comparison of clinicopathological characteristics between the pCR and non-pCR groups in the training and validation sets is shown in Table 1. In the training set, the median age was significantly higher in the pCR group than in the non-pCR group (55.6 vs 49.0 years old, $P = 0.008$). The mean largest tumor diameter in the pCR group was significantly smaller than that in the non-PCR group (6.5 vs 8.2 cm, $P = 0.007$). The most commonly used neoadjuvant conversion therapy was TACE + HAIC + TKI-ICIs in the pCR group and TACE alone in the non-PCR group (n=14, 51.9% vs n=20,

Table 1 Demographic and Clinical Characteristics of Patients in Each Cohort

Parameters	Training cohort (n=100)			Validation cohort (n=103)		
	PCR (n=27)	Non-pCR (n=73)	*P*-value	PCR (n=17)	Non-pCR (n=86)	*P*-value
Gender			0.722			1.000
Male	25(92.6%)	64(87.7%)		15(88.2%)	73(84.9%)	
Female	2(7.4%)	9(12.3%)		2(11.8%)	13(15.1%)	
Age,†	55.6(10.9)	49.0(10.2)	0.008	57.1(9.4)	52.0(12.1)	0.113
HBV/HCV infection			0.773			0.349
Negative	4(14.8%)	14(19.2%)		0(0.0%)	9(10.5%)	
Positive	23(85.2%)	59(80.8%)		17(100.0%)	77(89.5%)	
AFP (ng/mL)			0.131			0.003
≤ 200	21(77.8%)	45(61.6%)		17(100.0%)	57(66.3%)	
> 200	6(22.2%)	28(38.4%)		0(0.0%)	29(33.7%)	
ALT (U/L)			0.541			0.491
≤50	22(81.5%)	63(86.3%)		13(76.5%)	72(83.7%)	
>50	5(18.5%)	10(13.7%)		4(23.5%)	14(16.3%)	

(*Continued*)

Table 1 (Continued).

Parameters	Training cohort (n=100)			Validation cohort (n=103)		
	PCR (n=27)	Non-pCR (n=73)	*P*-value	PCR (n=17)	Non-pCR (n=86)	*P*-value
AST (U/L)			0.932			0.680
≤40	18(66.7%)	48(65.8%)		11(64.7%)	60(69.8%)	
>40	9(33.3%)	25(34.2%)		6(35.3%)	26(30.2%)	
GGT (U/L)			0.343			0.411
≤60	9(33.3%)	32(43.8%)		4(23.5%)	29(33.7%)	
>60	18(66.7%)	41(56.2%)		13(76.5%)	57(66.3%)	
ALB (g/L)			0.039			1.000
≤35	15(55.6%)	24(32.9%)		1(5.9%)	5(5.8%)	
>35	12(44.4%)	49(67.1%)		16(94.1%)	81(94.2%)	
TBIL (mg/dl)			0.384			1.000
≤17.1	24(88.9%)	58(79.5%)		15(88.2%)	76(88.4%)	
>17.1	3(11.1%)	15(20.5%)		2(11.8%)	10(11.6%)	
PT (s)			0.245			0.031
≤13	20(74.1%)	62(84.9%)		14(82.4%)	84(97.7%)	
>13	7(25.9%)	11(15.1%)		3(17.6%)	2(2.3%)	
Child-Pugh			0.294			1.000
A	25(92.6%)	71(97.3%)		17(100.0%)	85(98.8%)	
B	2(7.4%)	2(2.7%)		0(0.0%)	1(1.2%)	
Tumor number			0.297			0.392
Single	12(44.4%)	41(56.2%)		9(52.9%)	55(64.0%)	
Multiple	15(55.6%)	32(43.8%)		8(47.1%)	31(36.0%)	
Largest diameter of tumor (cm)†	6.5(3.0)	8.2(3.1)	0.007	5.4 (2.2)	6.6 (2.6)	0.048
BCLC stage			0.635			0.435
A	9(33.3%)	32(43.8%)		6(35.3%)	44(51.2%)	
B	9(33.3%)	20(27.4%)		6(35.3%)	26(30.2%)	
C	9(33.3%)	21(28.8%)		5(29.4%)	16(18.6%)	
Vascular invasion			0.719			0.241
Negative	19(70.4%)	54(74.0%)		13(76.5%)	76(88.4%)	
Positive	8(29.6%)	19(26.0%)		4(23.5%)	10(11.6%)	
MVI			0.725			0.067
Negative	25(92.6%)	65(89.0%)		17(100.0%)	70(81.4%)	
Positive	2(7.4%)	8(11.0%)		0(0.0%)	16(18.6%)	
Neoadjuvant conversion therapy strategy			0.029			0.137
TACE	3(11.1%)	20(27.4%)		2(11.8%)	13(15.1%)	
HAIC	0(0.0%)	1(1.4%)		6(35.3%)	50(58.1%)	
TACE+HAIC	2(7.4%)	7(9.6%)		2(11.8%)	9(10.5%)	
TACE+HAIC+TKIs/ICIs	14(51.9%)	17(23.3%)		3(17.6%)	8(9.3%)	
TACE+TKIs/ICIs	6(22.2%)	16(21.9%)		0(0.0%)	0(0.0%)	
HAIC+TKIs/ICIs	2(7.4%)	2(2.7%)		4(23.5%)	6(7.0%)	
Others	0(0.0%)	10(13.7%)		0(0.0%)	0(0.0%)	
CR evaluation by mRECIST			0.001			0.039
No	16(59.3%)	66(90.4%)		13(76.5%)	81(94.2%)	
Yes	11(40.7%)	7(9.6%)		4(23.5%)	5(5.8%)	

Notes: Values in parentheses are percentages unless indicated otherwise; †values are means (SD).

Abbreviations: HBV/HCV, hepatitis B/C virus; AFP, alpha-fetoprotein; ALT, alanine aminotransferase; AST, aspartate aminotransferase; GGT, γ-glutamyl transferase; ALB, albumin; TBIL, total bilirubin; PT, prothrombin time; BCLC, Barcelona Clinic Liver Cancer System; MVI, microvascular invasion; TACE, transarterial chemoembolization; HAIC, hepatic arterial infusion chemotherapy; TKIs, tyrosine kinase inhibitor; ICIs, immune checkpoint inhibitor; CR, complete response; mRECIST, modified Response Evaluation Criteria in Solid Tumors.

27.4%, $P = 0.029$). In the validation set, the proportion of AFP less than 200ng/mL in the pCR group was significantly higher than that in the non-PCR group (n=17, 100.0% vs n=57, 66.3%, $P = 0.003$). The mean largest tumor diameter in the pCR group was significantly smaller than that in the non-PCR group (5.4 vs 6.6 cm, $P = 0.048$). The most commonly used neoadjuvant conversion therapy was HAIC in both the pCR and non-PCR groups (n=6, 35.3% vs n=50, 58.1%; $P = 0.137$). A comparison of the baseline values between the two centers is presented in Table S1. The median largest tumor diameter in the training set was significantly larger than that in the validation cohort (7.5 cm vs 5.8 cm, $P = 0.002$). Preoperative CECT images of 27 patients (27.0%) in the training set indicated vascular invasion, which was significantly higher than that in the validation set (n=14, 13.6%; $P = 0.017$).

Consistency of Radiographic Complete Response and Pathological Complete Response

Of the 27 patients with pCR in the training set, only 11 underwent a preoperative mRECIST assessment of CR. The agreement rate between the two evaluation methods was 40.7%. Similarly, 4 of the 17 patients with pCR in the validation set had a preoperative mRECIST assessment of CR (Table 1 and Figure S1). This showed that the radiographic assessment of pCR was inaccurate.

The median follow-up duration for all the patients was 21.0 months. The median follow-up time for all patients was 21.0 months, and the RFS of the pCR subgroup was significantly better than that of the non-pCR subgroup in the training ($P = 0.005$, 2-year RFS: 68.8% and 31.5%, respectively; Figure 3A) and validation ($P = 0.045$, 2-year RFS: 70.6% and 39.6%, respectively; Figure 3B) sets.

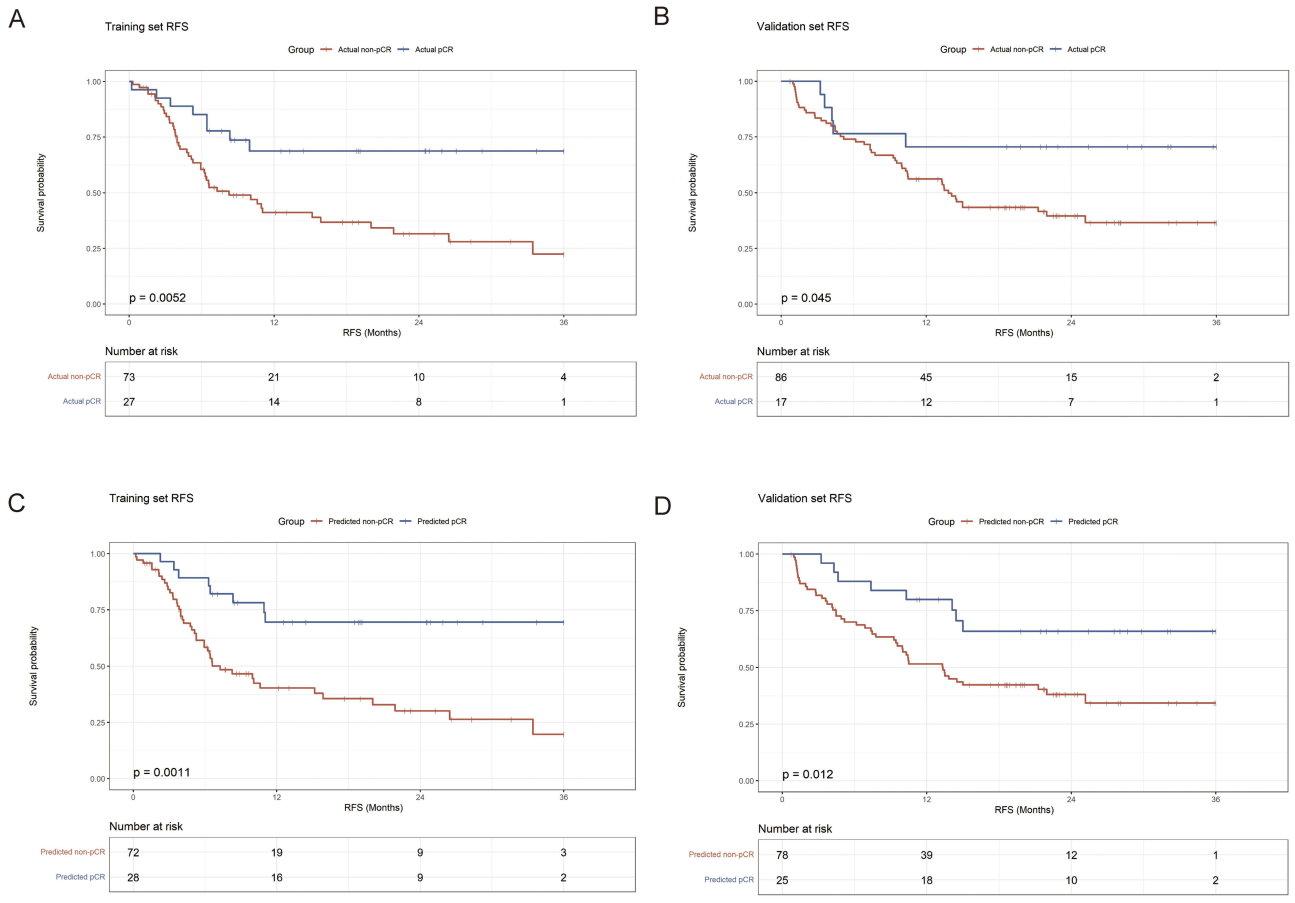

Figure 3 Kaplan-Meier RFS curves of actual pathological response subgroup and SMOTE-radiomic model predicted pathological response subgroup in two cohorts. Kaplan-Meier RFS curves of actual pathological response subgroup in training cohort (**A**) and validation cohort (**B**). Kaplan-Meier RFS curves of SMOTE-radiomic model predicted pathological response subgroup in training cohort (**C**) and validation cohort (**D**).

Abbreviations: pCR, pathological complete response; RFS, recurrence-free survival; SMOTE, synthetic minority over-sampling technique.

Radiomics Model Construction

A total of 396 radiomic features were extracted from the arterial and portal vein phases and 792 radiomic features were extracted from each patient (Table S2). The top ten important features (Table S3) were selected using the random forest algorithm, and the radiomics model was established using a logistic regression model. After balancing the training set using SMOTE, the number of patients in the SMOTE training set was 162 (81 pCR patients and 81 non-pCR patients). The SMOTE radiomics model was established based on the top 10 important features (Table S4) in the SOMTE training set using the random forest algorithm and a logistic regression model. In the training set, we found that age, mRECIST evaluation, and SMOTE-radiomics model were related to pCR (Table 2). We further explored whether the clinical-radiomics model constructed using these three factors had better predictive performance.

Performance of SMOTE-Radiomics Model

In the SMOTE-training training and validation sets, the AUC, accuracy, sensitivity, and specificity of the SMOTE radiomics model were 0.889, 0.843, 0.877, 0.864, 0.827, 0.824, 0.926, and 0.872, respectively (Figure 4). The AUC of 5-fold cross-validation of the SMOTE radiomics model in the SMOTE training set was 0.854, whereas the AUC of 5-fold cross-validation of the radiomics model in the original training set was 0.617. (Figure S2). The predictive performance of the radiomics model based on the original training set is shown in Figure S3. Compared to the radiomics model, the SMOTE radiomics model had a significantly higher predictive performance in the validation set (AUC: 0.655 vs 0.843, $P = 0.002$, Figure S3).

The AUC of both the SMOTE-radiomics and clinical-radiomics models were significantly better than those of the mRECIST model in both the training and validation sets (Figure 5). However, compared with the SMOTE-radiomics model, the AUC of the clinical-radiomics model did not significantly improve in the two cohorts (Figure 5). Therefore, we developed and validated an SMOTE radiomics model that can effectively predict postoperative pathological response.

Predictive Value of the SMOTE-Radiomics Model for RFS

As mentioned above, RFS of the pCR subgroup was significantly better than that of the non-pCR subgroup (Figure 3A and B). According to the cutoff value of 0.2109 in the SMOTE radiomics model, patients could be divided into predicted-pCR and predicted-non-pCR subgroups. The RFS of the predicted pCR subgroup was significantly better than that of the predicted non-pCR subgroup in the training cohort ($P = 0.001$, 2-year RFS: 69.5% and 30.1%, respectively; Figure 3C) and validation cohort ($P = 0.012$, 2-year RFS: 65.9% and 38.0%, respectively; Figure 3D). Cox multivariate analysis indicated that the pCR outcome predicted by the SMOTE-radiomics model was an independent factor for RFS in both the training (HR, 0.300; $P = 0.002$; Table 3) and validation sets (HR: 0.409, $P = 0.020$, Table 4).

Table 2 Univariate and Multivariate Analysis of Pathological Response in the Training Cohort

Variables	Reference	Univariable Analysis		Multivariable Analysis	
		OR (95% CI)	*P*-value	OR (95% CI)	*P*-value
Gender (Male vs Female)	Female	1.76 (0.35,8.71)	0.490		
Age (>60 vs ≤60 years)	≤60 years	2.99 (1.02,8.83)	0.047	2.71 (0.56,13.59)	0.215
HBV/HCV infection (Positive vs Negative)	Negative	1.36 (0.41,4.58)	0.615		
AFP (>200 vs ≤200 ng/mL)	≤200 ng/mL	0.46 (0.17,1.28)	0.136		
Tumor number (Multiple vs Single)	Single	1.60 (0.66,3.90)	0.299		
Largest diameter of tumor (>5 vs ≤5cm)	≤5 cm	0.47 (0.17,1.31)	0.148		
Vascular invasion (Positive vs Negative)	Negative	1.20 (0.45,3.18)	0.719		
CR evaluation by mRECIST (Yes vs No)	No	6.48 (2.17,19.35)	<0.001	6.65 (1.49,33.78)	0.016
SMOTE-radiomicsmodelpredictedoutcome(pCRvsNon-pCR)	Non-pCR	33.00 (9.98,109.11)	<0.001	34.72 (10.13,150.34)	<0.001

Abbreviations: OR (95% CI), odds ratio (95% confidence interval); HBV/HCV, hepatitis B/C virus; AFP, alpha-fetoprotein; CR, complete response; mRECIST, modified Response Evaluation Criteria in Solid Tumors; pCR, pathological complete response.

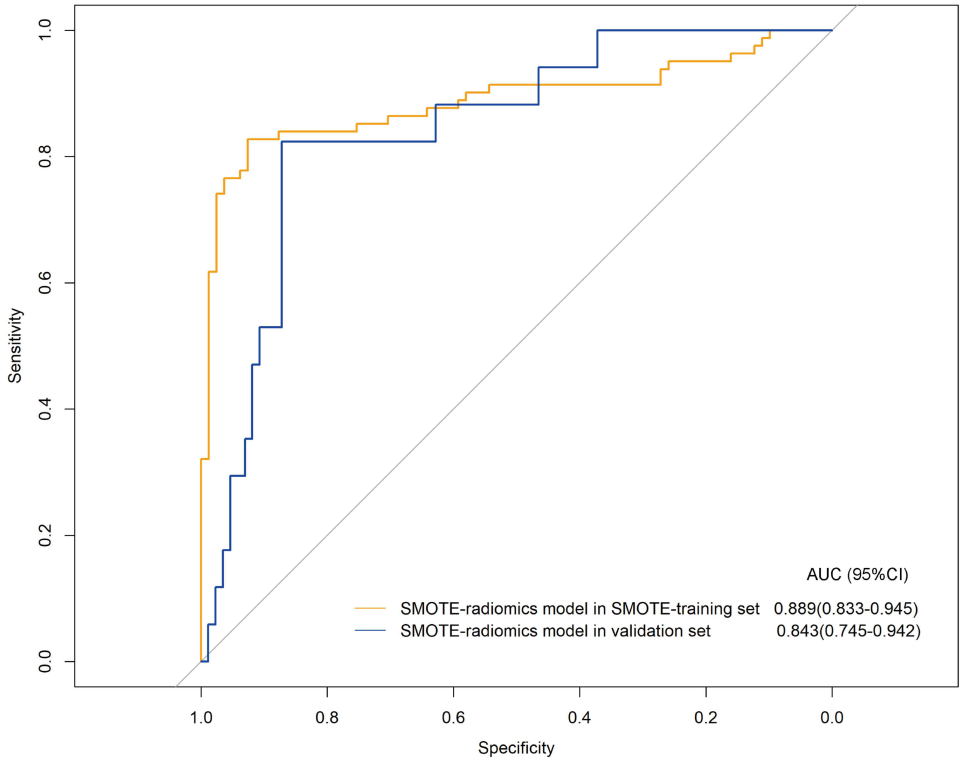

Cohort	Accuracy (%)	Sensitivity (%)	Specificity (%)
SMOTE-training set	87.7	82.7	92.6
Validation set	86.4	82.4	87.2

Figure 4 Performance of SMOTE-radiomics model in SMOTE-training set and validation set.
Abbreviations: AUC, area under the curve; SMOTE, synthetic minority over-sampling technique.

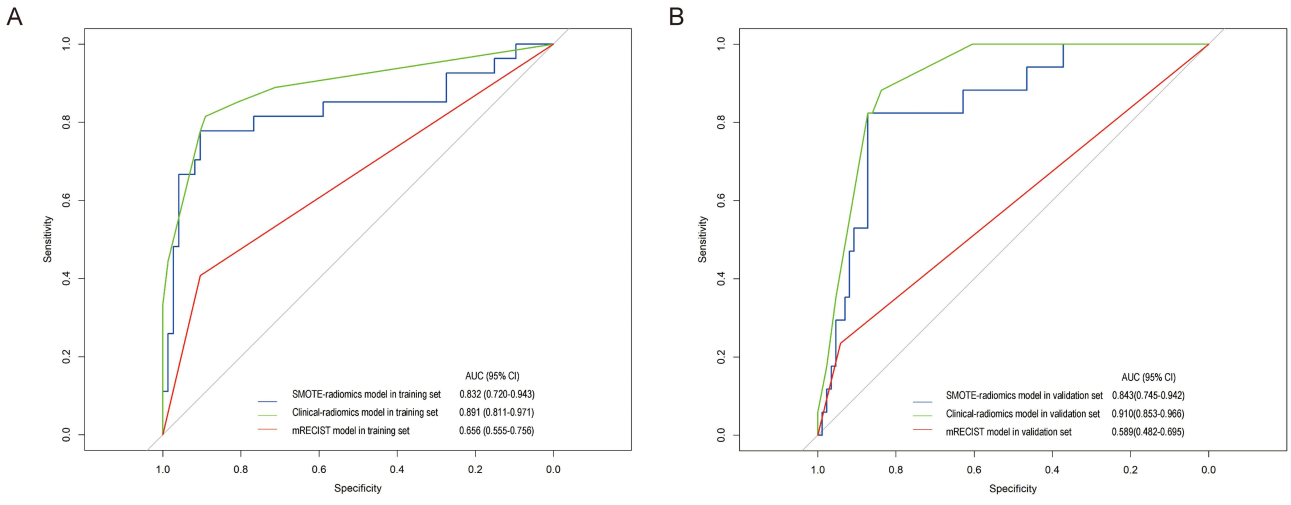

Figure 5 Comparison of the pCR-predicted performance of SMOTE-radiomics model, clinical-radiomics model and mRECIST model. (**A**) The ROC curves of three models in training set. SMOTE-radiomics model vs clinical-radiomics model, $P = 0.080$; SMOTE-radiomics model vs mRECIST model, $P = 0.020$; clinical-radiomics model vs mRECIST model, $P < 0.001$. (B) The ROC curves of three models in validation set. SMOTE-radiomics model vs clinical-radiomics model, $P = 0.300$; SMOTE-radiomics model vs mRECIST model, $P < 0.001$; clinical-radiomics model vs mRECIST model, $P < 0.001$.
Abbreviations: AUC, area under the ROC curve; SMOTE, synthetic minority over-sampling technique; pCR, pathological complete response; mRECIST, modified Response Evaluation Criteria in Solid Tumors; ROC, receiver operating curve.

Table 3 Univariate and Multivariate Analysis of RFS in the Training Cohort

Variables	Reference	Univariable Analysis		Multivariable Analysis	
		HR (95% CI)	*P*-value	HR (95% CI)	*P*-value
Gender (Male vs Female)	Female	0.89 (0.38,2.10)	0.793		
Age (>60 vs ≤60 years)	≤60 years	0.79 (0.37,1.68)	0.538		
HBV/HCV infection (Positive vs Negative)	Negative	1.51 (0.71,3.22)	0.282		
AFP (>200 vs ≤200 ng/mL)	≤200 ng/mL	1.11 (0.63,1.97)	0.715		
Tumor number (Multiple vs single)	Single	1.98 (1.15,3.44)	0.015	2.084 (1.201,3.616)	0.009
Largest diameter of tumor (>5 vs ≤5 cm)	≤5 cm	1.68 (0.79,3.58)	0.180		
Vascular invasion (Positive vs Negative)	Negative	1.00 (0.54,1.84)	0.997		
CR evaluation by mRECIST (Yes vs No)	No	0.42 (0.18,0.98)	0.045	0.524 (0.221,1.241)	0.142
SMOTE-radiomics model predicted outcome (pCR vs Non-pCR)	Non-pCR	0.30 (0.14,0.64)	0.002	0.300 (0.140,0.644)	0.002

Abbreviations: RFS, recurrence-free survival; HR (95% CI), hazard ratio (95% confidence interval); HBV/HCV, hepatitis B/C virus; AFP, alpha-fetoprotein; CR, complete response; mRECIST, modified Response Evaluation Criteria in Solid Tumors; pCR, pathological complete response.

Table 4 Univariate and Multivariate Analysis of RFS in the Validation Cohort

Variables	Reference	Univariable Analysis		Multivariable Analysis	
		HR (95% CI)	*P*-value	HR (95% CI)	*P*-value
Gender (Male vs Female)	Female	1.05 (0.50,2.22)	0.898		
Age (>60 vs ≤60 years)	≤60 years	0.69 (0.37,1.29)	0.243		
HBV/HCV infection (Positive vs Negative)	Negative	1.40 (0.51,3.88)	0.515		
AFP (>200 vs ≤200 ng/mL)	≤200 ng/mL	1.16 (0.64,2.10)	0.627		
Tumor number (Multiple vs single)	Single	2.33 (1.37,3.97)	0.002	2.267 (1.328,3.868)	0.003
Largest diameter of tumor (>5 vs ≤5 cm)	≤5 cm	1.49 (0.84,2.65)	0.169		
Vascular invasion (Positive vs Negative)	Negative	1.54 (0.77,3.05)	0.220		
CR evaluation by mRECIST (Yes vs No)	No	0.49 (0.15,1.58)	0.235		
SMOTE-radiomics model predicted outcome (pCR vs Non-pCR)	Non-pCR	0.39 (0.19,0.84)	0.015	0.409 (0.193,0.869)	0.020

Abbreviations: RFS, recurrence-free survival; HR (95% CI), hazard ratio (95% confidence interval); HBV/HCV, hepatitis B/C virus; AFP, alpha-fetoprotein; CR, complete response; mRECIST, modified Response Evaluation Criteria in Solid Tumors; pCR, pathological complete response.

Discussion

Based on data from 203 patients with initially unresectable HCC who underwent hepatectomy following neoadjuvant conversion therapy at two centers, we developed and validated a radiomics model based on CT radiomic features to predict the pathological response. In this study, the SMOTE radiomics model performed significantly better than the mRECIST assessment in the preoperative prediction of pCR. Furthermore, the pathological response predicted by the SMOTE radiomics model is an independent prognostic factor for RFS.

In China, 70–80% of patients with HCC reach the intermediate or advanced stage at the time of initial diagnosis and have lost the opportunity for radical surgery. Neoadjuvant conversion therapy, including locoregional and systemic treatments, can significantly improve the long-term benefits in patients with advanced HCC by transforming unresectable HCC into radically resectable HCC.[19–22] One of the most critical clinical issues for neoadjuvant conversion therapy is to evaluate whether pCR is achieved, which is an extremely important factor affecting the prognosis.[23–26] The mRECIST is one of the most commonly used criteria for evaluating tumor response in HCC preoperatively but with limited consistency with pathological results. The consistency rate of the mRECIST for evaluating CR with pCR was only 34.1% in this study, which is similar to a previous study.[9] The AFP level was reported to be associated with postoperative

pathological response in patients treated with TACE before surgery.[27] Therefore, efforts have been made to combine radiological and AFP responses to predicting pCR before surgery.[28] However, this study had a small sample size of only 35 patients, and lacked a validation cohort. Our SMOTE radiomics model showed good pCR-predictive performance in the training (AUC: 0.832) and validation cohorts (AUC: 0.843), which proved the universality of this model to some extent.

The significance of pCR evaluation was further verified in our study. Patients who achieved pCR after neoadjuvant conversion therapy showed a significantly better RFS than those who did not. Similarly, the SMOTE radiomics model could also stratify patients with advanced HCC receiving neoadjuvant conversion therapy into two prognostic subgroups with significantly different RFS. pCR group predicted by SMOTE-radiomics model had a longer RFS than non-pCR subgroup in both the training (mRFS: not reach vs 7.27 months, $P = 0.001$) and validation cohort (mRFS: not reach vs 13.3 months, $P = 0.012$). Therefore, we propose that the SMOTE radiomics model could serve as a preoperative risk stratification tool for treatment decision support.

In our study, ten radiomic features were used to establish the SMOTE radiomics model, five features were texture parameters, and three features were run-length matrix (RLM) parameters. ClusterShade_AllDirection_offset1_SD of the portal vein phase, a type of texture feature, is the most important feature of the SMOTE radiomics model. Texture parameters can represent the appearance of the tumor surface and its element distribution, and quantify the pixel intensity in cross-sectional imaging.[29,30] The RLM parameters reflect the heterogeneity of the images in different directions.[31] Texture and RLM reflect the heterogeneity of the signal intensity within the lesion. Some studies have demonstrated that texture and RLM on CT images can predict the treatment response of patients with HCC after TACE.[32,33] In addition, texture was associated with tumor grade and disease-free survival of HCC.[34] Neoadjuvant conversion therapy may result in reduced contrast between adjacent voxels in nontumor components, which can be reflected in the texture and RLM parameters. In this study, these two types of radiomic features were found to be closely related to the pathological response of tumors and prognosis in patients with advanced HCC.

We also constructed a clinical-radiomics model by adding pCR-related clinical factors, age, and mRECIST evaluation to the SMOTE-radiomics model; however, the predictive performance of the clinical-radiomics model did not improve significantly. The limited improvement in the addition of clinical factors, especially the mRECIST evaluation, might be due to their poor efficacy in predicting postoperative pCR. In this study, the AUCs of the mRECIST model for the training and validation sets were 0.656 and 0.589, respectively. Therefore, the SMOTE radiomics model itself is a good predictor of pCR.

Our study had several limitations. First, the data for the establishment of the SMOTE radiomics model were obtained from a retrospective cohort, which led to inevitable selection bias. Second, there were significant differences in neoadjuvant conversion therapy regimens between the two centers. However, the SMOTE radiomic model showed good predictive performance at both centers, proving the universality of this model. Third, owing to the limited number of patients included in the study, larger cohorts and prospective studies are needed in the future.

Conclusion

We established and validated a SMOTE radiomics model based on the radiomic features of CECT, which showed good performance in predicting the pathological response of unresectable HCC patients after neoadjuvant conversion therapy. Moreover, the pathological response predicted by the model was independently correlated with RFS. The model may have potential clinical value for clinical decision-making in neoadjuvant conversion therapy and for the selection of surgical timing.

Acknowledgment

This study was funded by the National Key Research and Development Program of China (2020AAA0109504), National Science Fund for Distinguished Young Scholars (81825013, 82322034), National Natural Science Foundation of China (82272942 and 82302283), Guangdong Natural Science Foundation of Distinguished Youth Scholar (No.2022B1515020060), Guangdong Natural Science Foundation (No. 2022A1515011716, No. 2022A1515010862),

Youth Fund of the National Natural Science Foundation of China (No. 81900546) and Sanming Project of Medicine in Shenzhen (No.SZSM202011010).

Disclosure

The authors report no conflicts of interest in this work.

References

1. Sung H, Ferlay J, Siegel RL, et al. Global Cancer Statistics 2020: GLOBOCAN Estimates of Incidence and Mortality Worldwide for 36 Cancers in 185 Countries. *CA Cancer J Clin*. 2021;71:209–249. doi:10.3322/caac.21660
2. Cherqui D, Laurent A, Mocellin N, et al. Liver resection for transplantable hepatocellular carcinoma: long-term survival and role of secondary liver transplantation. *Ann Surg*. 2009;250:738–746. doi:10.1097/SLA.0b013e3181bd582b
3. Roayaie S, Jibara G, Tabrizian P, et al. The role of hepatic resection in the treatment of hepatocellular cancer. *Hepatology*. 2015;62:440–451. doi:10.1002/hep.27745
4. Schlachterman A, Craft WJ, Hilgenfeldt E, Mitra A, Cabrera R. Current and future treatments for hepatocellular carcinoma. *World JGastroenterol*. 2015;21:8478–8491. doi:10.3748/wjg.v21.i28.8478
5. Hamaoka M, Kobayashi T, Kuroda S, et al. Hepatectomy after down-staging of hepatocellular carcinoma with portal vein tumor thrombus using chemoradiotherapy: a retrospective cohort study. *Int J Surg*. 2017;44:223–228. doi:10.1016/j.ijsu.2017.06.082
6. Zhu XD, Huang C, Shen YH, et al. Hepatectomy After Conversion Therapy Using Tyrosine Kinase Inhibitors Plus Anti-PD-1 Antibody Therapy for Patients with Unresectable Hepatocellular Carcinoma. *Ann Surg Oncol*. 2023;30(2782–2790):2782–2790. doi:10.1245/s10434-022-12530-z
7. Ho WJ, Zhu Q, Durham J, et al. Neoadjuvant Cabozantinib and Nivolumab Converts Locally Advanced HCC into Resectable Disease with Enhanced Antitumor Immunity. *Nat Cancer*. 2021;2:891–903. doi:10.1038/s43018-021-00234-4
8. Llovet JM, Lencioni R. mRECIST for HCC: performance and novel refinements. *J Hepatol*. 2020;72:288–306. doi:10.1016/j.jhep.2019.09.026
9. Bargellini I, Bozzi E, Campani D, et al. Modified RECIST to assess tumor response after transarterial chemoembolization of hepatocellular carcinoma: CT-pathologic correlation in 178 liver explants. *Eur J Radiol*. 2013;82:e212–e218. doi:10.1016/j.ejrad.2012.12.009
10. Limkin EJ, Sun R, Dercle L, et al. Promises and challenges for the implementation of computational medical imaging (radiomics) in oncology. *Ann Oncol*. 2017;28:1191–1206. doi:10.1093/annonc/mdx034
11. Aerts HJ, Velazquez ER, Leijenaar RT, et al. Decoding tumour phenotype by noninvasive imaging using a quantitative radiomics approach. *Nat Commun*. 2014;5:4006. doi:10.1038/ncomms5006
12. Sun R, Limkin EJ, Vakalopoulou M, et al. A radiomics approach to assess tumour-infiltrating CD8 cells and response to anti-PD-1 or anti-PD-L1 immunotherapy: an imaging biomarker, retrospective multicohort study. *Lancet Oncol*. 2018;19:1180–1191. doi:10.1016/S1470-2045(18)30413-3
13. Kickingereder P, Gotz M, Muschelli J, et al. Large-scale Radiomic Profiling of Recurrent Glioblastoma Identifies an Imaging Predictor for Stratifying Anti-Angiogenic Treatment Response. *Clin Cancer Res*. 2016;22:5765–5771. doi:10.1158/1078-0432.CCR-16-0702
14. Xu X, Zhang HL, Liu QP, et al. Radiomic analysis of contrast-enhanced CT predicts microvascular invasion and outcome in hepatocellular carcinoma. *J Hepatol*. 2019;70:1133–1144. doi:10.1016/j.jhep.2019.02.023
15. Liu F, Liu D, Wang K, et al. Deep Learning Radiomics Based on Contrast-Enhanced Ultrasound Might Optimize Curative Treatments for Very-Early or Early-Stage Hepatocellular Carcinoma Patients. *Liver Cancer*. 2020;9:397–413. doi:10.1159/000505694
16. Feng Z, Li H, Liu Q, et al. CT Radiomics to Predict Macrotrabecular-Massive Subtype and Immune Status in Hepatocellular Carcinoma. *Radiology*. 2023;307:e221291. doi:10.1148/radiol.221291
17. Chawla N, Bowyer K, Hall L, Kegelyemer W. SMOTE: synthetic Minority Over-sampling Technique. *J Artif Intell Res*. 2002;6:321–357. doi:10.1613/jair.953
18. Turhon M, Li M, Kang H, et al. Development and validation of a deep learning model for prediction of intracranial aneurysm rupture risk based on multi-omics factor. *Eur Radiol*. 2023;33:6759–6770. doi:10.1007/s00330-023-09672-3
19. Llovet JM, Ricci S, Mazzaferro V, et al. Sorafenib in advanced hepatocellular carcinoma. *N Engl J Med*. 2008;359:378–390. doi:10.1056/NEJMoa0708857
20. Kudo M, Finn RS, Qin S, et al. Lenvatinib versus sorafenib in first-line treatment of patients with unresectable hepatocellular carcinoma: a randomised Phase 3 non-inferiority trial. *Lancet*. 2018;391:1163–1173. doi:10.1016/S0140-6736(18)30207-1
21. Cheng AL, Kang YK, Chen Z, et al. Efficacy and safety of sorafenib in patients in the Asia-Pacific region with advanced hepatocellular carcinoma: a Phase III randomised, double-blind, placebo-controlled trial. *Lancet Oncol*. 2009;10:25–34. doi:10.1016/S1470-2045(08)70285-7
22. Forner A, Reig M, Bruix J. Hepatocellular carcinoma. *Lancet*. 2018;391:1301–1314. doi:10.1016/S0140-6736(18)30010-2
23. Allard MA, Sebagh M, Ruiz A, et al. Does pathological response after transarterial chemoembolization for hepatocellular carcinoma in cirrhotic patients with cirrhosis predict outcome after liver resection or transplantation? *J Hepatol*. 2015;63:83–92. doi:10.1016/j.jhep.2015.01.023
24. Blazer DR, Kishi Y, Maru DM, et al. Pathologic response to preoperative chemotherapy: a new outcome end point after resection of hepatic colorectal metastases. *J Clin Oncol*. 2008;26:5344–5351. doi:10.1200/JCO.2008.17.5299
25. Xu D, Liu XF, Yan XL, Wang K, Xing BC. Survival prediction in patients with resectable colorectal liver metastases: clinical risk scores and tumor response to chemotherapy. *Oncol Lett*. 2017;14:8051–8059. doi:10.3892/ol.2017.7191
26. Yamashita S, Chun YS, Kopetz SE, et al. APC and PIK3CA Mutational Cooperativity Predicts Pathologic Response and Survival in Patients Undergoing Resection for Colorectal Liver Metastases. *Ann Surg*. 2020;272:1080–1085.
27. Yang K, Sung PS, You YK, et al. Pathologic complete response to chemoembolization improves survival outcomes after curative surgery for hepatocellular carcinoma: predictive factors of response. *HPB*. 2019;21:1718–1726. doi:10.1016/j.hpb.2019.04.017
28. Huang C, Zhu XD, Shen YH, et al. Radiographic and alpha-fetoprotein response predict pathologic complete response to immunotherapy plus a TKI in hepatocellular carcinoma: a multicenter study. *BMC Cancer*. 2023;23:416. doi:10.1186/s12885-023-10898-z
29. Miles KA, Ganeshan B, Hayball MP. CT texture analysis using the filtration-histogram method: what do the measurements mean? *Cancer Imag*. 2013;13:400–406. doi:10.1102/1470-7330.2013.9045

30. Ganeshan B, Miles KA, Young RC, Chatwin CR. Texture analysis in non-contrast enhanced CT: impact of malignancy on texture in apparently disease-free areas of the liver. *Eur J Radiol*. 2009;70:101–110. doi:10.1016/j.ejrad.2007.12.005
31. Li Y, Xu X, Weng S, Yan C, Chen J, Ye R. CT Image-Based Texture Analysis to Predict Microvascular Invasion in Primary Hepatocellular Carcinoma. *J Digit Imaging*. 2020;33:1365–1375. doi:10.1007/s10278-020-00386-2
32. An H, Bhatia I, Cao F, Huang Z, Xie C. CT texture analysis in predicting treatment response and survival in patients with hepatocellular carcinoma treated with transarterial chemoembolization using random forest models. *BMC Cancer*. 2023;23:201. doi:10.1186/s12885-023-10620-z
33. Guo Z, Zhong N, Xu X, et al. Prediction of Hepatocellular Carcinoma Response to Transcatheter Arterial Chemoembolization: a Real-World Study Based on Non-Contrast Computed Tomography Radiomics and General Image Features. *J Hepatocell Carcinoma*. 2021;8:773–782. doi:10.2147/JHC.S316117
34. Oh J, Lee JM, Park J, et al. Hepatocellular Carcinoma: texture Analysis of Preoperative Computed Tomography Images Can Provide Markers of Tumor Grade and Disease-Free Survival. *Korean J Radiol*. 2019;20:569–579. doi:10.3348/kjr.2018.0501